*PROCEEDINGS OF THE INTERNATIONAL CONFERENCE NANOMATERIALS: APPLICATIONS AND PROPERTIES*
Vol. **2** No 3, 03NCNN07(6pp) (2013)

# The Role of Pore Structure of SMFs-based Pd Nanocatalysts in Deactivation Behavioral Pattern Upon Acetylene Hydrogenation Reaction

E. Esmaeili[1,2,3,*], A.M. Rashidi[3], Y. Mortazavi[2], A.A. Khodadadi[2], M. Rashidzadeh[3]

[1] *Birjand University of Technology, Department of Chemical Engineering, P.O. Box: 97175 / 569, Birjand, Iran*
[2] *Catalysis and Nanostructured Materials Research Laboratory, School of Chemical Engineering, University of Tehran, Tehran, Iran*
[3] *Research Institute of petroleum industry (RIPI), West Blvd. Azadi Sport Complex, P. O. Box: 14665-1998, Tehran, Iran*

(Received 01 May 2013; published online 29 August 2013)

In this research, SMFs panels were applied for further deposition of CNFs, ZnO and $Al_2O_3$ to hydrogenate selectively acetylene to ethylene. To understand the role of different structures of the examined supports, the characterization methods of SEM, ASAP, $NH_3$-TPD and $N_2$ adsorption-desorption isotherms were used. Following the characterization of green oil by FTIR, the presence of more unsaturated constituents and then, more branched hydrocarbons formed upon the reaction over alumina-supported catalyst in comparison with the ones supported on CNFs and ZnO was confirmed, which in turn, could block the pores mouths. Besides the limited hydrogen transfer, the lowest pore diameters of $Al_2O_3$ / SMFs close to the surface, supported by $N_2$ adsorption-desorption isotherms could explain the fast deactivation of this catalyst, compared to the other ones.

**Keywords:** Selective hydrogenation, Pore structure, SMFs-supported nanocatalysts, Deactivation.

PACS numbers: 82.65. + r, 87.16.dp

## 1. INTRODUCTION

In the recent decades, many global demands for ethylene-containing products have attracted so much attention [1]. Since, ethylene derived from the catalytic and/or thermal cracking of oil compounds includes small amounts of acetylene, selective hydrogenation of acetylene to ethylene is industrially suggested to purify ethylene feedstocks from traces of acetylene up to below 5 ppm [2-4]. In spite of the useless effect of alumina-supported catalysts at higher temperature, alumina is still used as the conventional support [5]. However, carbon-based supports have been extremely applied in selective hydrogenation reactions, as reported in literature [6-7]. Nowadays, some carbon supports such as carbon nanotubes and carbon nanofibers are competing with the oxide ones because of having interesting intrinsic characteristics which lead to more electron transfer and hydrogen spillover [8].

The using of some novel ordered supports such as monoliths [9], metallic grids [10], carbon fabrics [11] and bidimentional glass [12] in alkyne hydrogenation with high selectivity to alkenes has been shown better performance in comparison with the traditional reactors randomly filled with catalyst particles. Structured sintered metal fibers (SMFs), having the porosity of 80-90% and uniform fiber sizes of about several microns are very promising as catalytic supports due to interesting characteristics, i.e. high mechanical strength and thermal conductivity, large permeability and excellent filtrating properties with a low pressure drop through the catalytic bed, however, these supports have low surface area [13]. To increase the specific surface area (SSA) of the SMFs, the deposition of a micron layer of some well-known substrate may be proposed. In line with the above-mentioned advantages, some authors synthesized carbon nanofibers over SMFs via chemical vapor deposition (CVD) technique [14] to improve the specific surface area, which in turn, could decrease the run away during exothermic hydrogenation reactions [15]. Furthermore, they developed a structured catalyst including ZnO supported on SMFs to use in selective hydrogenation of 2- methyl-3-butyn-2-ol (MBY) to 2-methyl-3-buten-2-ol (MBE) [16].

Catalyst deactivation is one of the most important challenges in catalysis for many years. According to literature [17-21], both the structure and the nature of supports; i.e. pore configuration and acidity of the supports, respectively, could undergo the deactivation process as well. However, there are some challenges, especially, in the case of the role of acidic sites.

In the present study, the main objective of our study is to identify how the configuration and the nature of the support could influence the catalytic activity of Pd-based catalysts supported on CNFs / SMFs, $Al_2O_3$ / SMFs and ZnO / SMFs in selective hydrogenation reaction of acetylene.

## 2. MATERIALS AND METHODS

Commercially available Inconel sintered metal fibers ($SMF_{Inconel}$, Inconel 601, Bekipor ST20AL3, Bakaert Fiber Technology, Belgium) were used as a growth substrate for carbon nanofibers (CNFs). In order to clean the surface of the $SMFs_{Inconel}$ panels, they were calcined at 650 °C. The procedure of CNFs deposition over the panels has been already described elsewhere [14]. Briefly, CNFs were deposited on $SMFs_{Inconel}$ by the catalytic decomposition of ethane in the presence of hydrogen. Then, SMFs were treated by hydrogen (625 °C, 2 h, 120 cc/min) to decorate SMFs with Ni nanoparticles (SMFs is composed of an alloy mixture, containing nick-

* esmaeili@birjandut.ac.ir

 

el). Afterwards, the reactor was heated up to 675 °C, while, a mixture of Ar : $C_2H_6$ : $H_2$ = 80 : 3 : 17 (total flow rate of 600 cc/min) was passed through the reactor for 2 h. The resulted 5 wt % CNFs / SMFs composite supports were functionalized in a boiling 30 % $H_2O_2$ aqueous solution (Reactolab SA) for 1 h, followed by sonication in ethanol to remove amorphous carbon.

To prepare ZnO-based SMFs, we applied FeCrAl SMFs panels (40FP3, Southwest Screens & Filters, Bekaert SA, Belgium). Following the calcination of SMFs panels, appropriate amounts of zinc acetate dehydrate (Fluka) was added under vigorous stirring to the desired amounts of monoethanolamine (Fluka) and acetoin (Riedel-de Haen) dissolved in isopropanol [13]. Zinc oxide was deposited over the SMFs panels through dipping the SMFs substrates in the prepared solution. Afterwards, the resulted samples were dried using air at the ambient temperature for 0.5 h, followed by a rapid heating up to 600 °C. To reach up to ca. 5 wt % of ZnO over SMFs, we repeated the above procedure several times, consecutively. The last treatment was to increase the specific surface area of ZnO using the post-annealing the ZnO / SMFs supports at 900 °C.

Sintered Metal Fiber filters (40FP3 Stainless Steel, AISI316L, Southwest Screens & Filters, Bekaert SA, Belgium) was used to deposit $Al_2O_3$ over the SMFs panels. As mentioned previously, SMFs panels were treated prior to deposition of alumina, as described previously.

The desired amounts of $Al(NO_3)_3 \cdot 9\ H_2O$ (Aldrich) and anhydrous citric acid (Aldrich) dissolved in water were applied as the precursor solution to deposit alumina over SMFs panels. $Al_2O_3$ film deposition was performed via dipping, according to what explained for the ZnO-based samples, then drying the samples in air at room temperature, followed by the calcination at 600 °C (1 h, 5 °/min). The dipping-drying-calcination procedure was repeated several times to obtain the deposition weight of ca. 5 wt % $Al_2O_3$ on SMFs surface.

After cutting the prepared supports, wet impregnation method was applied to prepare Pd catalysts supported on CNFs, ZnO and $Al_2O_3$ fiber disks. Palladium acetate (Aldrich) dissolved in acetonitrile (Reactolab SA-1077 SERVION) was used as the precursor solution, adding to the samples in accordance with the weight porosity of the supports, i.e. 0.4 wt % with respect to the supports utilized. A mixture of argon and hydrogen was introduced into the reactor, passing over the disks for 2 h to reduce the catalysts.

Catalytic reactions were carried out in the reactor, while the reaction temperature was adjusted in the desired amount using oil circulating system. The reactant feedstocks containing 1.5 vol. % acetylene in 20 vol. % hydrogen diluted with argon (i.e. 78.5 vol. %), passing through the reactor was applied, whereas, the reaction temperatures of 120, 140 and 180 °C and the atmospheric pressure was used. The output gases were analyzed using HP 6890 gas chromatograph, supplied by a flame ionizer and a capillary column filled by Carboxen 1010.

The BET surface area and pore volume were measured by nitrogen adsorption at 77 K using an ASAP-2010 porosimeter from the Micromeritics Corporation GA. $NH_3$-TPD (Micromeretics 2900) was used to investigate the presence and the nature of acidic sites. Simulation Distillation (SIM DIS, Varian Simulated Distillation 5.5) analysis was applied to determine the amount of coke extracts, and also, to compare the nature of coke formed over the catalysts surfaces upon acetylene hydrogenation reaction. Carbon disulfide was used to extract the coke deposited on the catalysts aged during the reaction. FTIR (Bruker, Vertex 70) experiments were efficient to indicate the chemical nature of carbonaceous species formed. The surface morphology of the samples was investigated using SEM (JEOL JSM-6300F) instrument.

## 3. RESULTS AND DISCUSSION

Fig. 1 shows the catalytic activities of Pd catalysts at three different temperatures of 120, 140 and 180 °C. According to the figure, no distinct decrease in acetylene conversion for Pd / CNFs and Pd / ZnO supported on SMFs with time on stream is observed, meanwhile, Pd / $Al_2O_3$ shows a sharp decrease in catalytic performance, especially, at 180 °C, as it reaches up to the values even less than the ones obtained at 140 °C. Therefore, one may conclude that the increased temperature has a significantly positive role to enhance acetylene conversion except for the Pd / $Al_2O_3$ catalyst reacted at 180 °C. For instance, in the case of Pd / CNFs / SMFs, an increase of acetylene conversion from about 10 % at 120 °C to around 22 % at 180 °C is observed, respectively; however, the enhancement is more pronounced in the case of Pd / ZnO / SMFs catalyst. A considerable performance of Pd / ZnO / SMFs may be attributed to the formation of an effective interaction between Pd and Zn as PdZn alloy, as Semagina et al. have previously reported [13].

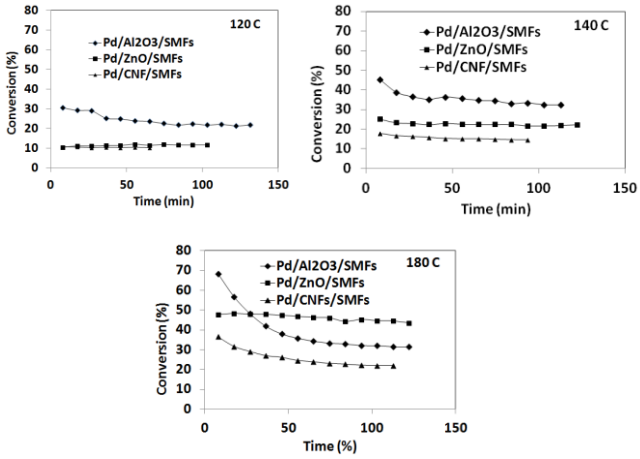


**Fig. 1** – Catalytic activities of SMF-supported Pd / CNFs, Pd / ZnO and Pd / $Al_2O_3$ catalysts at 120, 140 and 180 °C with time on stream in acetylene hydrogenation reaction (Total gas flow rate 400 cc/min)

Fig. 2 implies a comparative schematic of the selectivity to ethylene, ethane and undesired products (indicated as green oil (GO) in Fig. 2) at the reaction temperatures of 120, 140 and 180 °C. According to Fig. 2, the ethylene selectivity is enhanced with the increased temperature, for instance, the selectivity to ethylene is found to be about 76 % at 120 °C, whereas, it reaches up to ca. 91 % for ZnO-supported catalyst, forming less ethane and green oil at higher temperatures. As observed in Fig. 2, ZnO-supported Pd catalyst exhibits the highest selectivity to ethylene and the lowest selectivity to ethane and green oil in comparison with the ones of CNFs- and $Al_2O_3$-supported Pd catalysts.

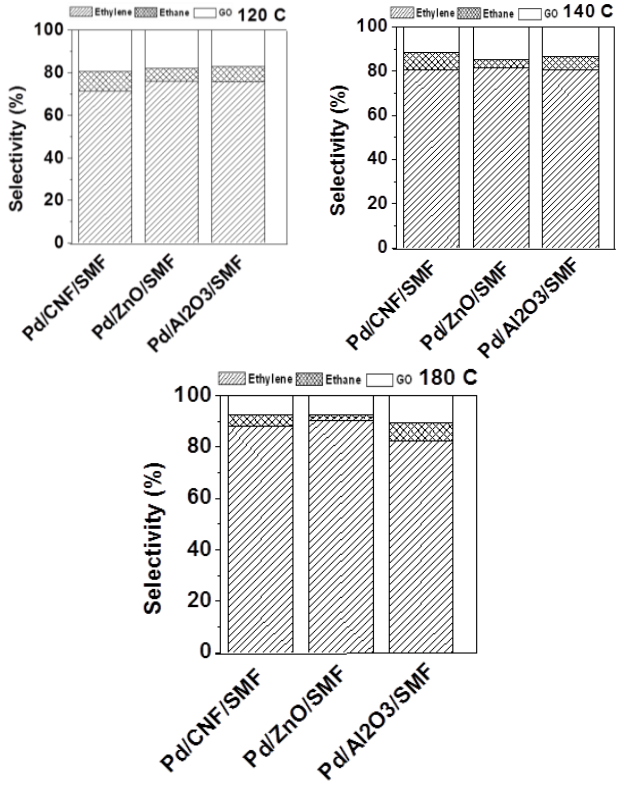


**Fig. 2** – The variation of selectivities to ethylene, ethane and green oil (GO) vs. reaction temperature

Fig. 3 presents the SEM micrographs of $SMFs_{Inconel}$ and $SMFs_{FeCrAl}$ (Figs. 3a and c) in the oxidized state and after deposition of CNFs and ZnO (Figs. 3b and d) supports over them. According to Figs. 3a and c, the diameter of $SMFs_{Inconel}$ is found to be ca. 8-10 μm, whereas, in the case of $SMFs_{FeCrAl}$, it is found to be around 15-20 μm. Considering Fig. 3b, one may observe a porous support, having Ni nanoparticles segregated to the surface of $SMFs_{Inconel}$. According to Fig. 3, the SEM photographs of Figs. 3b and d indicates higher roughness and lower surface area for the ZnO / SMFs sample in contrary to the CNFs / SMFs one.

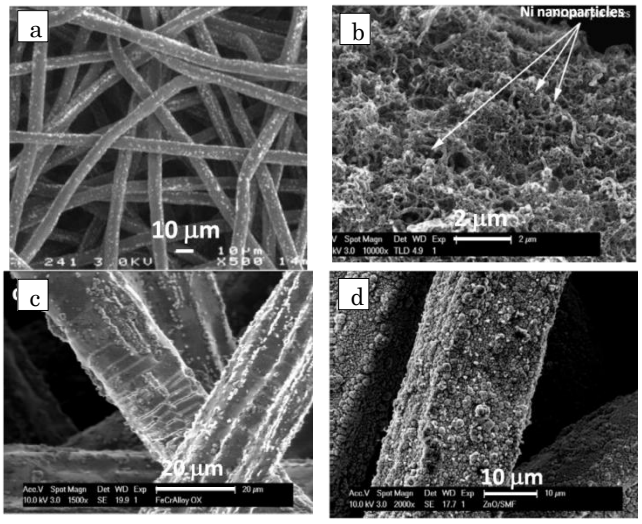


**Fig. 3** – SEM micrographs of a) $SMFs_{Inconel}$, b) CNFs/SMFs, c) $SMFs_{FeCrAl}$, d) ZnO/SMFs

FTIR results of the green oil extracted from the catalysts aged for 8 h upon the reaction are shown in Fig. 4. Taking into account to the figure, one may conclude that the bands appeared at around 2854 and 2926 $cm^{-1}$ and at ca. 2873 and 2955 $cm^{-1}$ are respectively associated with the vibration modes of $CH_2$ and $CH_3$ groups in the oligomeric chains [22-23]. According to FTIR spectra, the lowest relative ratio of intensities of $CH_2$ / $CH_3$ is associated with the coke resulted from Pd / $Al_2O_3$ / SMFs, i.e. the lower chain length of the green oil upon the reaction is formed over SMFs-supported Pd / $Al_2O_3$, however, the amount of coke is more pronounced for this catalyst, when it is compared with the other catalysts examined (see Fig. 2).

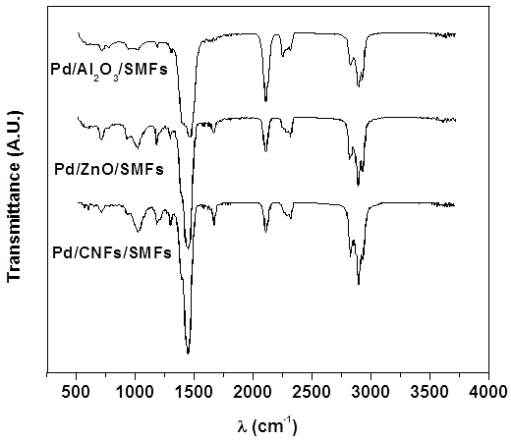


**Fig. 4** – FTIR spectra of extracted green oil of SMFs-supported Pd / CNFs, Pd / ZnO and Pd / $Al_2O_3$ catalysts after 8 h under acetylene hydrogenation reaction (Total gas flow rate = 400 cc/min, $T$ = 180 °C).

The presence of C ≡ C bond is confirmed by the band indicated at 2296 $cm^{-1}$ and also, more drastically at 2155 $cm^{-1}$ [24]. According to the figure, the peak located at 2155 $cm^{-1}$ is very sharp for the extracts resulted from the Pd / $Al_2O_3$, while, the corresponding ones belonged to Pd / ZnO and Pd / CNFs are found to be less intensified.

The peak centroid at around 1640 $cm^{-1}$ is assigned to C = C bond (i.e. olefins) [25]. According to the figure, higher intensity of C = C bond is belonged to the spectra of green oil resulted from Pd / CNFs and Pd/ZnO, when it is compared with that of the Pd / $Al_2O_3$. Moreover, the band revealed at 1450 $cm^{-1}$ could confirm the presence of higher intensities of C = C groups for the green oil resulted from Pd / CNFs and Pd / ZnO compared to that of Pd / $Al_2O_3$ [26].

All the documents mentioned above could be a confirmation to prove the presence of higher amounts of hydrogen in the coke formed over the SMFs-supported Pd / CNFs and Pd / ZnO, when they are compared with the one of Pd / $Al_2O_3$ / SMFs catalyst. This could guide us towards the hydrogen transfer as the governing mechanism in acetylene hydrogenation reaction. Therefore, a small rate of hydrogen transfer via the hydrocarbon layer is expected, leading to more unsaturated species and likely more branching of the green oil extracted from the aged catalyst of Pd / $Al_2O_3$ / SMFs than those of SMFs-based Pd / CNFs and Pd / ZnO. More branched hydrocarbons, more steric hinderance and less accessibility of the reactants to the active sites [27].

In the present study, ZnO / SMFs support doesn't show any clear peaks in $NH_3$-TPD (not shown here), however, according to Fig. 1; Pd / ZnO / SMFs catalyst presents good catalytic performances. It seems that there is no distinct correlation between the presence of acidic sites and deactivation rate of the catalyst. This idea may be more emphasized, when the behavior of Pd / $Al_2O_3$ / SMFs catalyst are taken into account, having some acidic sites (not shown here) along with very fast deactivation.

The role of acidic sites in deactivation process is discussing as a major challenge for many years. In spite of some authors [28-30] who emphasized a direct correlation between the number of acidic sites and the amounts of coke formation, there are some opposite theories in literature [31-32]. According to them [31-32], deactivation process was explained through blocking rather than consumption or poisoning of the acidic sites.

Fig. 6 depicts the $N_2$ adsorption-desorption isotherms of SMFs-based CNFs, ZnO and $Al_2O_3$ supports. The isotherms associated with both oxide supports (i.e. ZnO and $Al_2O_3$ supported on SMFs) are indicative of Type II isotherms, implying non-porous or macroporous supports along with the hysteresis loop of Type H3, i.e. characteristics of aggregates of plate-like particles, leading to slit-shaped pores [33-34].

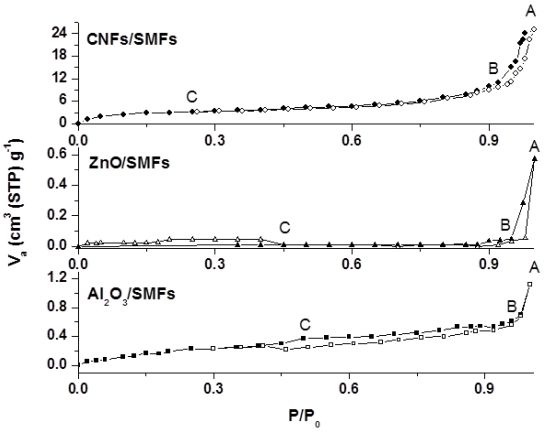


**Fig. 6** – $N_2$ adsorption-desorption isotherms of the SMFs-supported $Al_2O_3$, ZnO and CNFs (empty symbols: adsorption, full symbols: desorption)

According to Fig. 6, one may observe that Type IV isotherm is the characteristic feature of CNFs-containing SMFs which in turn, indicates capillary condensation, taking place in mesopores. The initial part of the Type IV isotherm up to C point is attributed to monolayer-multilayer adsorption; however, it is followed by the same propensity as the corresponding one of a Type II isotherm associated with the non-porous form [33-34]. Type H1 belonged to the porous materials is in accordance with the feature of SMFs-supported CNFs sample [33-34].

As known, in the course of ascending isotherm of the adsorption branch, the first vertical rise in volume is indicative of the size of nanochannels in capillary condensation. From Fig. 6, the larger size of nanochannels is found for the ZnO-containing SMFs support. Upon descending, the rapid decrease from A to B reflects the macropore of interparticle voids. Therefore, the presence of a severe slope in desorption branch from A to B for both SMFs-based oxides is confirmed, in contrast to the one of CNFs-included. According to literature [35], one may conclude that lower amount of liquid nitrogen evaporation from B to C is attributed to the pore-blocking effect in the defective voids which is more significant for SMFs-supported $Al_2O_3$ than the one of ZnO. Since, the pore blocking effect decreases because of higher concentrations of voids exposed to the external surface, one may conclude that higher desorption of nitrogen and subsequently, more voids close to the external surface for the ZnO / SMFs in comparison with the ones of $Al_2O_3$-based support is expected. Although the driving force required for the opening-up of the interconnecting channels between voids, i.e. from point C towards the completely desorption of nitrogen for the CNFs / SMFs and $Al_2O_3$ / SMFs, is still existed, no distinct decrease in the case of ZnO / SMFs is found [35].

Based on what explained above, an evaluation of pore analysis of all supports is required to identify the surface characteristics of the supports for better explanation of their catalytic behavior. The physical characteristics of the SMFs-supported CNFs, ZnO and $Al_2O_3$ are exhibited in Table 1. According to Table 1, the highest value of BET surface area is found to be 213.9 $m^2/g$ for the CNFs / SMFs sample, whereas, the lowest one is associated with the ZnO / SMFs, i.e. 3.3 $m^2/g$. Mean pore diameter are corresponding to 14.7, 18.2 and 6.4 nm, respectively, assigned to the SMFs-supported CNFs, ZnO and $Al_2O_3$.

**Table 1** – Some intrinsic physical characteristics of CNFs, ZnO and $Al_2O_3$ supported on SMFs

| Support | BET surface area[a] ($m^2/g$) | BET surface area[b] ($m^2/g$) | Pore diameter (nm) |
|---|---|---|---|
| CNFs / SMFs | 10.27 | 213.9 | 14.7 |
| ZnO / SMFs | 0.148 | 3.3 | 18.2 |
| $Al_2O_3$ / SMFs | 0.893 | 19.8 | 6.4 |

[a]BET surface area of the composite
[b]BET surface area without considering the SMFs

According to FTIR spectra and Table 1, one may conclude that the shorter chain length of the coke extracts of Pd / $Al_2O_3$ is in accordance with the smaller pore diameter of this catalyst [36-37]. In addition to the presence of the larger pore diameters in Pd / CNFs / SMFs and Pd / ZnO / SMFs, these supports have different results of ammonia desorption (mentioned previously). As reported in literature [36-37], the dimensions of the coke formed upon aging are mainly affected by the dimensions of the pore structure of the catalyst. Dimon et al. [37] investigated the effect of zeolite structures in deactivation behavior, when propene gas was passed over it. According to them, the hydrogen transfer mechanism was more pronounced in the case of USHY than that of HZSM-5 zeolite, because the coke related to the former catalyst was contained 3 and 4 unsaturations in comparison with the latter one with 0, 1 and 2 unsaturations, i.e. the branching degree was more significant with USHY than the HZSM-5. In line with them, the differences occurred for two mentioned catalysts could be attributed to the diversities in the pores sizes. Moreover, some indicative observations have been reported based

on which the pore diameter of the mesoporous supports such as MCM-41 played a sensitive role to influence the catalytic activities. It is of great importance to note that MCM-41with larger pore sizes compared to zeolites improves the catalytic activity of the reaction, facilitating the accessibility of the reactants to the active sites [38]. To investigate the effect of pore size, He et al. [38] compared the catalytic activity of [Si,Ti]-MCM-41 with silicalite I. They rationalized that the former catalyst is more effective due to its larger pores diameters. Besides the results mentioned, considering the results of Reddy and co-workers [39] may be of interest. According to them, the conversion of real petroleum resid feed was more significant for normal-loading Co-MoS / $Al_2O_3$ compared to that of high-loading CoMoS / MCM-41. They concluded, however, that this was attributed to the smaller pores diameters and thus, the lowered accessibility of the active phase of CoMoS / MCM-41 compared to the mean pores diameters of the CoMoS / $Al_2O_3$, i.e. 2.34 nm in contrast to 10.5 nm, respectively.

According to what resulted from Fig. 6, one may conclude that for the ZnO / SMFs support, more macropores are exposed to its external surface, when it is compared with those of $Al_2O_3$ / SMFs which in turn, facilitate the diffusion of branched-chain oligomers, as reported previously [40]. Since, the maximum kinetic diameter of the oligomers is ca. 1 nm, using a support with larger pore diameter is required. According to Fig. 6, one may conclude that the major contribution of the macropores takes place far from the external surface of SMFs-supported alumina, having the smaller pores mouths (may be lower than 1 nm) exposed to the surface which in turn, facilitates the catalyst deactivation upon the reaction.

However, the reaction rate is the highest with Pd / $Al_2O_3$ / SMFs (78 mol / mol of Pd.s) compared to Pd / CNFs (32 mol / mol of Pd.s) and Pd / ZnO (49 mol/mol of Pd.s), the narrower pores diameters of $Al_2O_3$ / SMFs sample may be responsible for the steric hindrance, more branching and subsequently, faster deactivation of the catalyst in comparison with the larger ones of CNFs / SMFs and ZnO / SMFs samples [20, 37]. According to the findings resulted from the current study, one may conclude that the mechanism of deactivation upon acetylene hydrogenation reaction may be affected by the hydrogen transfer, forming highly-branched and/ or less-saturated oligomers spelt over from the catalyst surface towards the support which in turn, could blocks the smaller pores of the catalyst.

## 4. CONCLUSION

SMFs-supported CNFs, ZnO and $Al_2O_3$ were applied to study the effect of support structure on deactivation behavioral pattern in acetylene hydrogenation reaction. Pd / ZnO / SMFs exhibited the best catalytic performance along with the highest stability compared to the other catalysts examined, especially at higher temperatures. Considering the results of catalytic activity and $NH_3$-TPD of the catalysts, one might conclude that acidity has no indicative effect in catalyst deactivation. FTIR results of the coke formed over Pd / $Al_2O_3$ / SMFs confirmed the formation of more branched hydrocarbons containing the higher percentage of unsaturated bonds in comparison with the ones formed over ZnO- and CNFs-supported Pd catalysts. The presence of more branched hydrocarbons could be responsible for catalyst deactivation as a result of pore blocking. According to the findings resulted from the current study, pore blocking had more significant effect in deactivation of Pd-based alumina catalyst, having the lowest pore diameter, i.e. the dimensions of the pores could affect the rate of catalyst deactivation.

## AKNOWLEDGEMENTS

The helpful supports of Professor L. Kiwi-Minsker and her group in EPFL (GGRC) is greatly appreciated.

## REFERENCES

1. K. Kovnir, M. Armbrüster, D. Teschner, T. Venkov, L. Szentmiklosi, F. Jentoft, A. Knop-Gericke, Y. Grin, R. Schlögl, *Surf. Sci.* **603**, 1784 (2009).
2. J. Panpranot, K. Kontapakdee, P. Praserthdam, *Appl. Catal. A* **314**, 128 (2006).
3. J. Kang, E. Shin, W. Kim, J. Park, S. Moon, *Catal. Today* **63**, 183 (2000).
4. J. Kang, E. Shin, W. Kim, J. Park, S. Moon, *J. Catal.* **208**, 310 (2002).
5. P. Praserthdam, B. Ngamsom, N. Bogdanchikova, S. Phatanasri, M. Pramotthana, *Appl. Catal. A* **230**, 41 (2002).
6. Y. Ryndin, M. Stenin, A. Boronin, V. Bukhtiyarov, V. Zaikovskii, *Appl. Catal.* **54**, 277 (1989).
7. H. Bazzazzadegan, M. Kazemeini, A. Rashidi, *Appl. Catal. A* **399**, 184 (2011).
8. E. Diaz, M. Leon, S. Ordonez, *Int. J. Hydrogen Energy* **35**, 4576 (2010).
9. T. Nijhuis, G. Koten, J. Moulijn, *Appl. Catal. A* **238**, 259 (2003).
10. J. Reymond, D. Dubois, P. Fouilloux, *Stud. Surf. Sci. Catal.* **118**, 63 (1998).
11. V. Höller, K. Radevik, I. Yuranov, L. Kiwi-Minsker, A. Renken, *Appl. Catal. B* **32**, 143 (2001).
12. E. Joannet, C. Horny, L. Kiwi-Minsker, A. Renken, *Chem. Eng. Sci.* **57**, 3453 (2002).
13. N. Semagina, M. Grasemann, N. Xanthopoulos, A. Renken, L. Kiwi-Minsker, *J. Catal.* **251**, 213 (2007).
14. P. Tribolet, L. Kiwi-Minsker, *Catal. Today* **102**, 15 (2005).
15. M. Ruta, I. Yuranov, P. Dyson, G. Laurenczy, L. Kiwi-Minsker, *J. Catal.* **247**, 269 (2007).
16. M. Crespo-Quesada, M. Grasemann, N. Semagina, A. Renken, L. Kiwi-Minsker, *Catal. Today* **147**, 247 (2009).
17. C. Bartholomew, *Appl. Catal. A* **212**, 17 (2001).
18. D. Blackmond, J. Goodwin, J. Lester, *J. Catal.* **78**, 34 (1982).
19. H. Karge, *Stud. Surf. Sci. Catal.* **58**, 531 (1991).
20. E. Gamas, I. Schifter, *Stud. Surf. Sci. Catal.* **111**, 119 (1997).
21. J. Bai, S. Liu, S. Xie, L. Xu, L. Lin, *Stud. Surf. Sci. Catal.* **147**, 715 (2004).
22. F. Geobaldo, G. Spoto, S. Bordig, C. Lamberti, A. Zecchina, *J. Chem. Soc. Faraday Trans.* **93**, 1243 (1997).
23. A. Dogan, G. Siyakus, F. Severcan, *Food Chem.* **100**, 1106 (2007).
24. D. Pavia, G. Lampman, G. Kriz, *Introduction to Spectroscopy: A Guide for Students of Organic Chemistry* (Glendale: Thomson Learning Inc: 2001)

25. R. Cicero, M. Linford, C. Chidsey, *Langmuir* **16**, 5688 (2000).
26. A. Gayubo, J. Arandes, A. Aguayo, M. Olazar, J. Bilbao, *Ind. Eng. Chem. Res.* **32**, 588 (1993).
27. B. Langner, *Ind. Eng. Chem. Process Des. Dev.* **20**, 326 (1981).
28. F. Fajula, F. Gault, *J. Catal.* **68**, 291 (1981).
29. F. Fajula, F. Gault, *J. Catal.* **68**, 312 (1981).
30. B. Langner, S. Meyer, *Stud. Surf. Sci. Catal.* **6**, 91 (1980).
31. H. Karge, E. Boldingh, *Catal. Today* **3**, 53 (1988).
32. D. Eisenbach, E. Gallei, *J. Catal.* **56**, 377 (1979).
33. K. Sing, D. Everett, R. Haul, et al., *Pure Appl. Chem.* **57**, 603 (1985).
34. C. Sangwichien, G. Aranovich, M. Donohue, *Colloid. Surf. A* **206**, 313 (2002).
35. H. Lin, S. Wong, C. Mou, C. Tang, *J. Phys. Chem. B* **104**, 8967 (2000).
36. P. Menon, *Chem. Rev.* **94**, 1021 (1994).
37. B. Dimon, P. Cartraud, P. Magnoux, M. Guisnet, *Appl. Catal. A* **101**, 351 (1993)
38. J. He, W. Xu, D. Evans, X. Duan, C. Li, *Microporous Mesoporous Mater.* **44**, 581 (2001).
39. K. Reddy, B. Wei, C. Song, *Catal. Today* **43**, 261 (1998).
40. V. Hulea, F. Fajula, *J. Catal.* **225**, 213 (2004).